Langmuir

Article

pubs.acs.org/Langmuir

Heteroprotein Complex Coacervation: Bovine β-Lactoglobulin and Lactoferrin

Yunfeng Yan,[†,‡] Ebru Kizilay,*[,†,∥] Daniel Seeman,[†] Sean Flanagan,[†] Paul L. Dubin,*[,†] Lionel Bovetto,[§] Laurence Donato,[§] and Christophe Schmitt[§]

[†]Department of Chemistry, University of Massachusetts Amherst, Amherst, Massachusetts 01003, United States

[‡]Department of Chemistry, Shanghai Normal University, Shanghai 200234, China

[§]Department of Food Science and Technology, Nestlé Research Center, Vers-chez-les-Blanc, CH-1000 Lausanne 26, Switzerland

[∥]Department of Chemical Engineering, Massachusetts Institute of Technology, Cambridge, Massachusetts 02139, United States

Supporting Information

ABSTRACT: Lactoferrin (LF) and β-lactoglobulin (BLG), strongly basic and weakly acidic bovine milk proteins, form optically clear coacervates under highly limited conditions of pH, ionic strength I, total protein concentration C_P, and BLG:LF stoichiometry. At 1:1 weight ratio, the coacervate composition has the same stoichiometry as its supernatant, which along with DLS measurements is consistent with an average structure $LF(BLG_2)_2$. In contrast to coacervation involving polyelectrolytes here, coacervates only form at I < 20 mM. The range of pH at which coacervation occurs is similarly narrow, ca. 5.7−6.2. On the other hand, suppression of coacervation is observed at high C_P, similar to the behavior of some polyelectrolyte−colloid systems. It is proposed that the structural homogeneity of complexes versus coacervates with polyelectrolytes greatly reduces the entropy of coacervation (both chain configuration and counterion loss) so that a very precise balance of repulsive and attractive forces is required for phase separation of the coacervate equilibrium state. The liquid−liquid phase transition can however be obscured by the kinetics of BLG aggregation which can compete with coacervation by depletion of BLG.

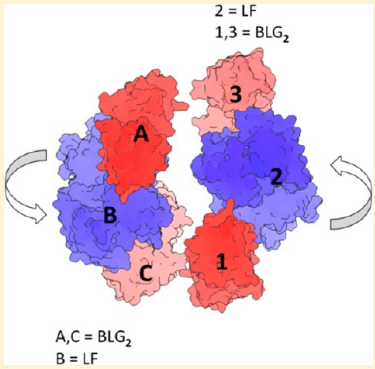

INTRODUCTION

Heteroprotein coacervation is a largely unexplored phenomenon at the interface of protein chemistry and colloid physics, appearing in a rather fragmented way in the contexts of food science, protein purification, or novel biomaterials. Despite some resemblance to the interactions of cognate proteins, heteroprotein coacervation resembles more nearly other forms of intermacroionic coacervation. While association of cognate proteins may have an electrostatic component, noncognate pairs lack the variety of short-range interactions providing cognate specificity. In contrast, the critical role of pH seen for heteroprotein liquid−liquid phase separation[1,2] suggests a predominant role of protein charge that is more in accord with Coulombic attractions and counterion release associated with complex coacervation. Typical complex coacervation however, nearly always involves flexible chain polyelectrolytes, so that the coacervation of a pair of globular proteins with constrained structural features would have to impose restrictions on both coacervation conditions and the coacervate structure. While coacervation may coexist with protein aggregation, heteroprotein coacervation is not subject to kinetic control, but rather exhibits equilibrium liquid−liquid phase separation, and is fully reversible (putting aside the instability of the metastable suspension of droplets often referred to as the "coacervate"). Just as coacervation is being recognized as a route to new soft materials,[3] coacervates of lactoferrin and β-lactoglobulin studied here may be of interest in new food products.

Heteroprotein association differs from native state protein self-aggregation in two important aspects: the type of kinetics and the pH-dependence of the resultant structure. While both the aggregation process and the final aggregate structures are governed by electrostatic interactions in both systems, due to nonequilibrium nature of self-aggregation, the resultant phases might be different. Protein native state self-aggregation typically observed at low salt concentrations and at pH near pI,[4] is a kinetically controlled process, and the resultant aggregates are typically fractal objects, which form nonordered and often irreversible structures. Native state protein aggregation is usually subject to salt-suppression in contrast to denatured aggregation. While denatured aggregation is almost always irreversible, the initial steps of native state aggregation are reversible. In many proteins, heat-induced misfolding leads to formation of β-sheet-rich fibrillar aggregates. On the other hand, heteroprotein association can lead to formation of ordered structures. Self-assembly of oppositely charged proteins

Received: July 18, 2013
Revised: October 11, 2013
Published: October 28, 2013

has in the past decade been involved in "bottom-up" fabrication of nanomaterials. For example, protein scaffolds with different morphology and functionality could be generated from globular proteins (e.g., yeast prion protein). The relative rigidity of both partners in heteroprotein coacervation simplifies modeling and simulations. However, heteroprotein coacervation has been the subject of very little attention, perhaps because the requisite conditions are highly limiting.

Three specific contrasts between heteroprotein coacervation and the behavior of other oppositely charged macroion pairs deserve further explanation. (a) Coacervation for PE−PE, PE−protein, and PE−micelle systems can occur at ionic strengths I as large as 400 mM,[5,6] while heteroprotein coacervation pairs have only been reported at I < 20 mM.[1,2] (b) The range of bulk charge stochiometry ([+]/[−]) in which coacervation can occur for PE-containing systems may be broad,[6] but heteroprotein coacervation occurs over a narrow range of [+]/[−]. (c) For PE−colloid and PE−PE systems, the predominant requirement for maximum coacervation is [+]/[−] close to 1; for heteroprotein systems, an additional requirement of "size compensation" appears, that is, maximum coacervation (e.g., "formation of microspheres") only occurs when the size or the sum of size of positively charged proteins is equal to those of negatively charged proteins.[1] There are several obvious reasons for these distinctions. (a) The high charge density and chain flexibility of PEs facilitate extensive ion-pairing which accounts for the salt-resistance of PE−PE or PE−colloid coacervate. (b) The heterogeneity of polycations or polyanions with respect to chain length or charge density, absent for globular proteins, can lead to complexes that achieve electroneutrality in various ways under different conditions of pH or bulk stoichiometry. (c) In PE-PE systems, coacervated complementary chains, well-mixed on submolecular length scales, can be ion-paired to achieve electroneutrality even if [+]/[−] ≠ 1; for heteroprotein systems, charge neutrality can only be attained on a length scale larger than protein size and is controlled by the geometry of protein packing, an effect separate from [+]/[−]. The way in which charges are mixed, that is, "ion-pairing", has two aspects, an enthalpic contribution and entropy of counterion release, which often drives PE−PE and PE−colloid coacervation.[6,7] PE−colloid systems occupy an intermediate role between PE−PE and heteroprotein systems in which the entropic role of counterion release must be even more severely diminished. The reduction in entropic driving forces for heteroprotein interactions results in coacervation conditions that are even more constrained.

Despite the differences note above, both heteroprotein and polyelectrolyte-protein systems are governed by electrostatics, which in turn depends on the ionic strength and the pH-dependent protein charge. The magnitude of these interactions in both systems determines whether soluble complexes, coacervate or precipitate is formed. This has in particular been demonstrated for systems involving the milk proteins α-lactalbumin (ALA), BLG, and lactoferrin (LF), specifically ALA and lysozyme,[2,8−10] lysozyme and BLG,[11] and ALA and LF.[12] The association of globular proteins lysozyme (Lys) and α-lactalbumin (ALA) at pH 7.5 in solution decreases with increase in ionic strength I, being completely abolished at I = 100 mM.[2] Observations for this system by turbidity, zeta potential and optical microscopy reveal that pH, by changing protein charge, controls formation of soluble complexes, coacervate, and precipitate.[13,14] Lactoferrin, a strongly basic milk protein, is obviously susceptible to interactions with acidic milk proteins such as ALA at a physiological ionic strength.[12] These LF−ALA interactions highly depend on ionic strength and more concentrated systems are required for complexation when I = 0. Interactions also occur between LF and unfolded proteins, coacervating with bovine casein fractions, and binding to native micellar caseins[15,16] and urea-denatured ALA.[12] For example, while not explicitly designated as such, previous studies in all likelihood contained examples of heteroprotein complex coacervation.

Here we examine in detail the interactions and phase separation behavior of two milk proteins. BLG is an intensively studied milk protein, and, as a major component of whey, of great interest in food science. Lactoferrin is a uniquely basic iron-binding protein of the transferrin family, with important biological functions in human milk, especially colostrum.[17−19] Lactoferrin and β-Lactoglobulin appear to be capable of heteroprotein liquid phase separation[1,14] via their interaction at pH's intermediate between their respective isoelectric points, 8.7.[4,16] and 5.2.[20] In the present work, complex formation and coacervation were studied as a function of pH, ionic strength, total protein concentration, and stoichiometry for mixtures of β-lactoglobulin (BLG, 18.4 kDa, pI ∼ 5.2) and lactoferrin (LF, 80 kDa, pI ∼ 8.7). The well-studied and explicit structures of both proteins facilitate modeling for the heteroprotein coacervation comprised of two globular proteins. We used turbidimetric titrations, direct observation after centrifugation, and dynamic light scattering (DLS) to explore conditions required for both precipitation (self-aggregation) and coacervation. DLS and size exclusion chromatography (SEC) were used to characterize the one-phase system at conditions of heteroprotein interaction, and supernatant from centrifugation. Based on the results obtained, boundary conditions leading to BLG−LF coacervations have been compared to those reported for polyelectrolyte-based coacervating systems.

EXPERIMENTAL SECTION

Materials. Bovine β-lactoglobulin powder (BLG from Davisco Foods International, Inc., batch number: JE 001−8−415) and lactoferrin powder (LF, from DMV, batch number: 10444427) were supplied by Nestlé Research Center (Lausanne, Switzerland). The powder composition was the following (g/100g wet powder): BLG is composed of BLG-A (55.4%), BLG-B (41.6%), and α-lactalbumin (1.6%). BLG: Na 0.554, K 0.004, Mg 0.002, Ca 0.018, P 0.054, Cl 0.047, protein 89.3 (Kjeldhal, Nx6.38) of which 97% was β-lactoglobulin; LF: Na 0.087, K 0.001, Mg 0.0003, Ca 0.002, Fe 0.014, P 0.021, Cl 0.920, protein 93.1 (Kjeldhal, Nx6.38) of which 97% was lactoferrin.[16] Lactoferrin is an iron-containing protein with a molecular mass of 76−80 kDa with 2 Fe^{3+} binding centers. Its red/orange color due to iron absorption. Milli-Q water was used in all sample preparation.

BLG−LF Complex Formation/Coacervation. Stock solutions of each protein were prepared in Milli-Q water with concentrations of 100.0 g/L. BLG−LF mixtures were prepared by three methods. For "pH-first", solutions were diluted and adjusted to a target I and pH using a NaCl (4.0 M) stock solution and 1.0 N standard NaOH or HCl. 5.0 mL of LF stock solution was rapidly poured into an equal volume of freshly prepared BLG solution in a 15 mL centrifuge tube followed by vortexing for 10 s and then centrifuging for 30 min at 3200g. For "high to low", BLG and LF solutions at pH 8.0 were mixed and then the mixtures were rapidly adjusted to a target pH while vortexing followed by centrifugation. For "low to high", BLG and LF solutions were mixed at pH 3.0 and then the mixtures were adjusted to a target pH quickly while vortexing, followed by centrifugation. The total protein concentration was kept constant at 20 g/L in all I, pH and BLG:LF dependence studies. All experiments were performed at 25 °C.

dx.doi.org/10.1021/la4027464 | Langmuir 2013, 29, 15614−15623

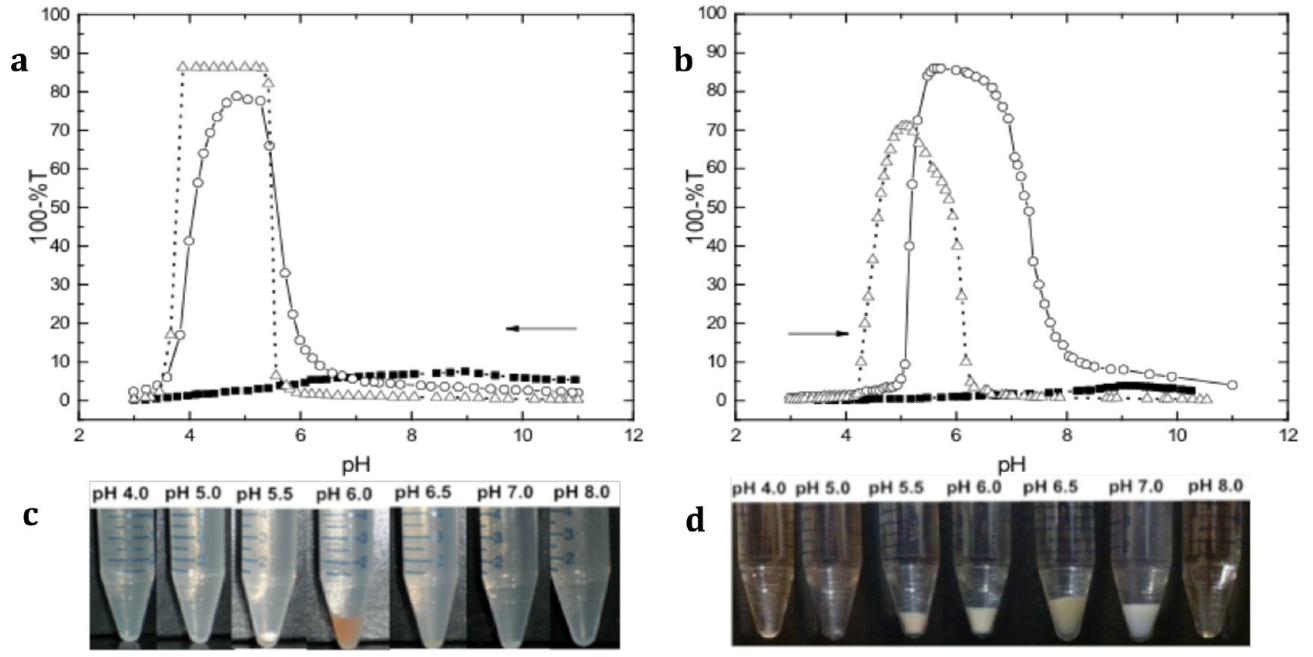

Figure 1. (a, b)Turbidimetric titration of 20 g/L BLG−LF mixture (○), 10 g/L BLG (△), and 10 g/L LF (■) in pure water (a) with 0.1 N HCl and (b) with 0.1 N NaOH. (c, d) Phase separation in BLG−LF, observed after centrifugation at 3200*g* for 30 min. (c) "High to low" procedure: mixed at pH 8, then adjusted with HCl to the target pH. (d) "Low to high" procedure: mixed at pH 3, then adjusted with NaOH to target pH. Neither aggregation nor complexation occurs in the regions of extreme pH (<4.0 or >10.0). DLS measurements (not shown) indicate that LF structure is unperturbed at pH 11.

Turbidimetric Measurements. Transmittance of protein solutions was measured using a Brinkmann PC 800 colorimeter equipped with a 520 nm filter and a 2.0 cm path length fiber optics probe, calibrated to 100% transmittance with Milli-Q water. Instrument drift after a 30 min warm-up was less than 0.1% T hr^{-1}. Turbidity was reported as 100-T% which is essentially linear with true turbidity τ for $\%T > 90$. pH was measured with a Corning 240 pH meter calibrated with pH 4.0 and 7.0 buffers. For pH/turbidimetric titration ("type 1 titration"), BLG (20 g/L) and LF (20 g/L) were mixed at 1:1 (v:v) at pH 11.0. Such a high pH was chosen to ensure the absence of LF aggregate, and was found by DLS measurements at pH 8 to give an identical result as an initial pH of 10. 0.1 N HCl was then added to the mixture with stirring and simultaneous monitoring of pH and transmittance. Titrations of individual proteins at 10 g/L were performed as controls. For the titration of BLG with LF ("type 2 titration"), a solution of 100 g/L LF with a microburet to 15 mL of 1.0 g/L BLG at pH 6.0 in 0−10 mM. The time between additions was kept at 30 s and $\%T$ was recorded before each addition.

Dynamic Light Scattering. (DLS). DLS was performed with a Malvern Zetasizer ZS instrument equipped with a 633 nm He−Ne laser and aligned for backscattering at 173°. Assuming diffusive relaxations, translational diffusion coefficients (D_T) were obtained from the fitting of DLS autocorrelation functions with non-negative constrained least-squares (NNLS). D_T can be further converted into hydrodynamic radius ($R_h = kT/(6\pi\eta D_T)$), where k is the Boltzmann constant, T is absolute temperature, and η is solvent viscosity.

Size Exclusion Chromatography (SEC). BLG−LF mixtures were equilibrated for 30 min after mixing, centrifuged at 3700 rpm (3200*g*) for 30 min, and the supernatant was taken for SEC analysis. Protein concentration was determined directly for the supernatant using a Superose 6 HR column on a Shimadzu Prominence LC system with 50 μL injections and a flow rate of 0.3 mL/min, while the protein content of the dense phase was determined by difference. The optimized eluant was 30 mM sodium phosphate, in 470 mM NaCl at pH 8.5. BSA (68.5 kDa), ovalbumin (44 kDa), carbonic anhydrase (29 kDa), ribonuclease A (13.7 kDa), and acetone were used for calibration. The concentrations of each protein was calculated from working curves in the range of 0.1−10 g/L. Detection was by absorbance at λ = 280 nm.

■ RESULTS AND DISCUSSION

The effect of pH, ionic strength, total protein concentration and weight mixing ratio were investigated in order to determine the boundary conditions leading to BLG−LF complex coacervation. Special emphasis was given to possible coupling between BLG self-aggregation and BLG−LF coacervation.

1. Effect of pH. *1.1. Turbidimetric Titrations.* In the present work, we find that self-aggregation (particularly that of BLG) can and often does obscure or interfere with coacervation. For this reason, we performed turbidimetric pH titrations in order to discriminate between kinetically controlled self-aggregation (the only turbidimetrically observed event for protein alone), and effects due to BLG−LF interaction appearing in the mixture, possibly accompanied by protein self-aggregation. Since turbidity does not always distinguish between liquid−liquid (coacervation) and liquid−solid (precipitation) phase separation, we centrifuged samples prepared at selected pH's by the same titration process, i.e. addition of acid or addition of base. In Figure 1a, the turbidimetric pH dependence for BLG−LF, obtained by titration with HCl is compared to that for BLG and LF alone. The maximum in turbidity for BLG at 3.5 < pH < 5.7 due to self-aggregation typically displayed at pH less than pI (5.2), e.g. in the range of 3.7 < pH < 5.2 for 1 g/L BLG at low salt[21] is here amplified by high concentration. Self-aggregation of LF on a much smaller scale is observed at pH 8−10, the region below pH 8 corresponding to disaggregation. Titration of the mixture can be considered in terms of three possibilities: (a) the turbidity of the mixture is the sum of the individual turbidities and we can assume that BLG−LF interactions are negligible; (b) the turbidity of the mixture exceeds the sums of the individual

dx.doi.org/10.1021/la4027464 | *Langmuir* 2013, 29, 15614−15623

protein contributions, i.e. BLG−LF interactions cause greater association or aggregation; and (c) the mixture turbidity is less than the individual sums, and either BLG is suppressing LF aggregation or LF is suppressing BLG aggregation. Case (a) appears so infrequently as to be adventitious; case (b) is seen at pH 5.7−6.2. case (c) is seen at 7.5 < pH < 10.0 where BLG suppresses LF aggregation, and at 4 < pH < 5 where LF suppresses BLG aggregation. This is consistent with the images of centrifuged samples (Figure 1c) where BLG precipitate is seen only at pH 5.5, small in magnitude compared to the extensive BLG aggregation seen at pH 5.5 or 6.0 in Figure 1d (to be discussed below). The gradual increase in turbidity for BLG−LF beginning at pH ∼ 6.5 and progressing rapidly at pH < 6.0 (particularly at pH 5.7−6.2) cannot be attributed to LF for which turbidity diminishes in this range, but must be due to the formation of BLG−LF complexes subject to one or more equilibria. In Figure 1c, it becomes evident that coacervate precursors must have been present at pH ∼ 6.5 but that BLG aggregation is not fully suppressed, as evident from the appearance of coacervate without BLG aggregation in Figure 2 (pH 6.0) to be discussed below.

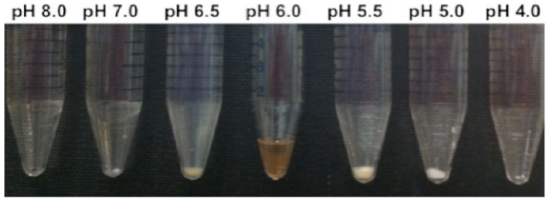

Figure 2. Phase separation in BLG−LF, prepared by "pH-first" procedure, observed after centrifugation at 3200*g* for 30 min. Results similar to that at pH 6.0 were obtained for pH = 5.8−6.2.

Comparison of the turbidimetric titrations seen with HCl with results for titration with NaOH in Figure 1b provides complementary information about the interplay of aggregation and complexation. The pH of maximum aggregation rate for BLG alone at about 4.9[4,21] in Figure 1a and b shows that the pH condition at which turbidimetric rates of BLG aggregation and disaggregation compensate each other is not strongly dependent on path, but the asymmetries are different in that the ascending side (aggregation) is steeper than the descending side for the titration from low to high pH (disaggregation slower than in titration with HCl).[21] The inhibiting role of LF on BLG aggregation due to complex formation is clearly seen at pH 4−5 as the onset aggregation is advanced from pH 4.1 to 5 in the presence of LF. But separate roles of complexes and BLG aggregates at pH > 5.0 cannot be resolved by turbidity. Figure 1d at pH 5.5, however, shows dramatic enhancement of BLG aggregate vs Figure 1c at the same pH. Although LF inhibits BLG aggregation in the region 5.0 < pH < 5.5, large and increasing levels of BLG precipitate, sometimes mixed with LF, are seen in Figure 1d as the pH increases from 5.5 to 6.5. With adjustment from low to high pH, precipitation of BLG clearly wins the competition with coacervation as a result of passing through maximum aggregation states. BLG precipitate persists even at pH 7.0, a condition at which BLG fails to aggregate alone or in the presence of LF. In summary, the effect of titration direction (Figure 1a vs b) is consistent with different pH profiles for aggregation and complex formation. This may also be revealed by the appearance of the dense phase arrived at by different modes of pH adjustment, one of which might be able to minimize aggregation as shown below. Interestingly, such a coupling between BLG self-aggregation and coacervation had been already reported in presence of gum arabic at pH 4.2.[22,23] Upon mixing of a protein dispersion containing both native and partially unfolded protein, the resulting mixture exhibited BLG aggregates coated with gum arabic together with BLG/gum arabic coacervates. Removal of partially unfolded BLG by isoelectric precipitation led to a purely complex coacervation between the two macromolecules. These findings also resemble previous ones describing the ability of LF to inhibit aggregation of urea-unfolded ALA at neutral pH[12] and even dissociate electrostatically bridged native milk casein micelles.[16]

BLG−LF coacervation can be decoupled from BLG self-aggregation only if the sample does not pass through aggregation states as occurred in the titrations of Figure 1. Results for the solutions rapidly adjusted to the desired pH (from pH 7 for BLG, and from pH 5 for LF), and then mixed are shown in Figure 2. The "pH-first" method leads to formation of a complex coacervate unique to this procedure at pH = 6.0. Coacervation is favored by the presence of aggregate-free solutions in which there are enough proteins (e.g., BLG dimers) to form the BLG−LF complexes required for coacervation. On the other hand, samples obtained at pH 5.0 and 5.5 exhibit precipitates because pH adjustment of BLG alone from pH 7.0 to pH 5.5 or 5.0 leads to BLG aggregation (Figure 1a for BLG alone) too abruptly to be excluded by rapid adjustment from pH 7.0. As will be discussed below, the images of Figure 2 should not be taken to imply infinitely narrow pH conditions for coacervation (see Figure S4 in the Supporting Information).

1.2. DLS of One-Phase and Supernatant Systems. To verify the tentative assignments of macroscopic turbidity data to protein self-aggregation or coacervation, we turn to DLS measurements in Figure 3 corresponding to the one-phase samples (open symbols) or supernatants (filled symbols) in Figures 1c,d and 2. Turning first to the preparation of samples by titration with HCl, Figure 1a and c identified the pH region 5.7−6.2 (where the turbidity is larger than the sum of the two individual proteins) as that of association arising from BLG−LF interactions. The presence of coacervate in tube 4 in Figure 1c indicates that the turbidity arose from coacervate droplets whose sedimentation leaves behind a supernatant with only the 22 nm BLG−LF complex presumably in equilibrium with coacervate. There is no evidence of BLG or its aggregate in this supernatant. The region where pH ≥ 6.5 could be identified from Figure 1a and c as one in which aggregation of LF exceeds that of BLG, and the modes at 120 (seen in pure LF) and 15 nm (not seen in pure LF) and LF aggregate and BLG−LF complex, respectively. Similarly, Figure 1a at pH 7 shows that the turbidity of the mixture can be largely due to LF aggregation, consistent with the 150 and 10 nm species (LF aggregate and monomer) both in pure LF at this pH (Figure S1, Supporting Information).

To understand the role of complex formation in the aggregation observed at pH > 5.0, the species present in the "one-phase" or supernatant samples shown in Figure 1d can be identified from the DLS results in Figure 3. In Figure 1b, the BLG−LF mixture titrated with NaOH exhibits high turbidity from 5.0 to 7.5. The onset of aggregation in the mixture occurs at a higher pH value than for BLG alone, which starts to aggregate at pH 4.1. This pH shift is due to the inhibiting role of LF on BLG aggregation via complex formation. As expected,

dx.doi.org/10.1021/la4027464 | *Langmuir* 2013, 29, 15614−15623

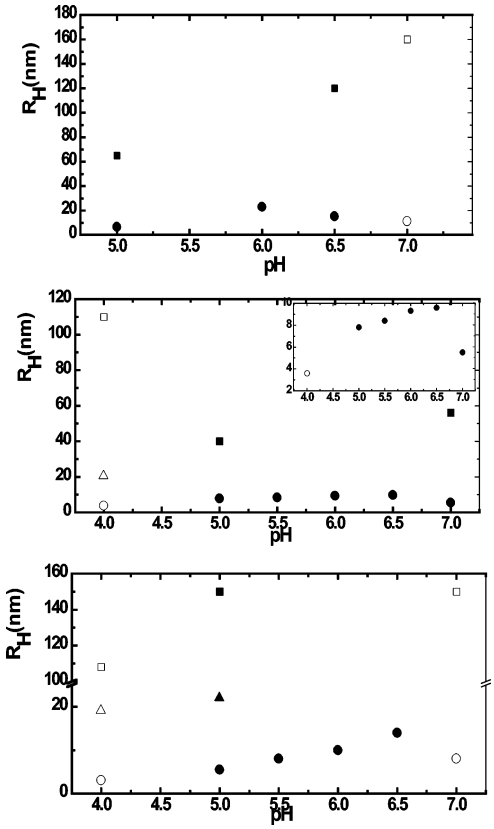

Figure 3. Evolution of hydrodynamic radius R_h of complexes present in one phase or supernatants obtained from samples shown in Figure 2. (top) "High to low" procedure; (middle) "low to high" procedure; (bottom) "pH-first" procedure. Filled symbols, supernatants; open symbols, one-phase. Circles, triangles and squares are fast, intermediate, and slow modes, respectively. Soluble BLG–LF complexes (7 nm < R_H < 22 nm) are kinetically stable and resistant to sedimentation over 2 h (see text).

the supernatant obtained after NaOH adjustment to pH 5.0. The sample shown Figure 1d contains <50 nm BLG–LF complexes (Figure 3, middle), which apparently do not proceed to form coacervate due to competition with BLG aggregation which depletes free BLG. Time-dependent DLS of the system at pH 5.0 (not shown here) shows a 100 nm slow mode which increases over 1 h to 600 nm, along with time-independent 7 and 40 nm objects that can be identified as stable complexes. Species with R_h of 7–10 nm seen in the supernatants at 5.0 < pH < 6.5 can be attributed to BLG–LF complexes; this is because LF does not aggregate at this pH range, and BLG aggregation does not lead to any stable intermediate species between dimer and larger aggregates.[4] Continuous increase in size of such complexes from 7 to 10 nm (Figure 3, middle, inset) suggests that they associate to form BLG–LF aggregates that coprecipitate with BLG aggregates. Unlike BLG aggregates, which acquire excess charge at pH 7, BLG–LF aggregates do not dissolve at this pH (Figure 1d). At pH 7.0, such BLG–LF aggregates are less soluble than they were at pH 6.5, and no longer remain in the supernatant.

As noted above, protein self-aggregation competes with complexation, which is needed to form precursors of coacervation. In order to examine this effect, DLS was used to compare species in the supernatants with complexes observed in the titrations of Figures 2. Species with size ~10 nm in the supernatant of coacervate formed at pH 6.0 ("pH first") (Figure 3, bottom) are similar to complexes seen in "high to low" (Figure 3, top). These species are believed to be the precursors of ~22 nm complexes seen in the supernatant of turbid coacervate (Figure 1c). The absence of complexes at pH 5.0 in the supernatants of Figure 2 can be attributed to reduction of the number of BLG dimers by aggregation during adjustment to that target pH. On the other hand, the "pH-first" procedure that leads to pure coacervate yields supernatant at 5.5 < pH < 6.5 containing BLG–LF complexes with R_h of 7–12 nm. Aggregate-free solutions that form a sufficient number of BLG–LF complexes can proceed to pure coacervate.

2. Effect of Ionic Strength. Figure 4 highlights the effect of changing of added-salt (0–100 mM) used in sample preparation on phase separation of BLG and LF at pH 5.9 (prepared by "pH first"). Figure 4c shows a rapid decrease in protein yield at $I \geq 20$ mM, consistent with the volume decrease from 8 to 2.5% for $I > 20$ mM seen in Figure 4a, with BLG:LF molar ratios (4 ± 0.5):1. Dense phases obtained at 100 > $I \geq 5$ mM are less fluid, and appear as white precipitates at 100 mM > I > 10 mM, pointing to predominance of BLG precipitate. The samples in Figure 4a have distinctly different histories, so neither these images nor the plot of Figure 4 should imply transitions from one equilibrium state to another with increasing or decreasing I. The aggregation rate of BLG at fixed pH increases strongly with decreasing salt[11] and its

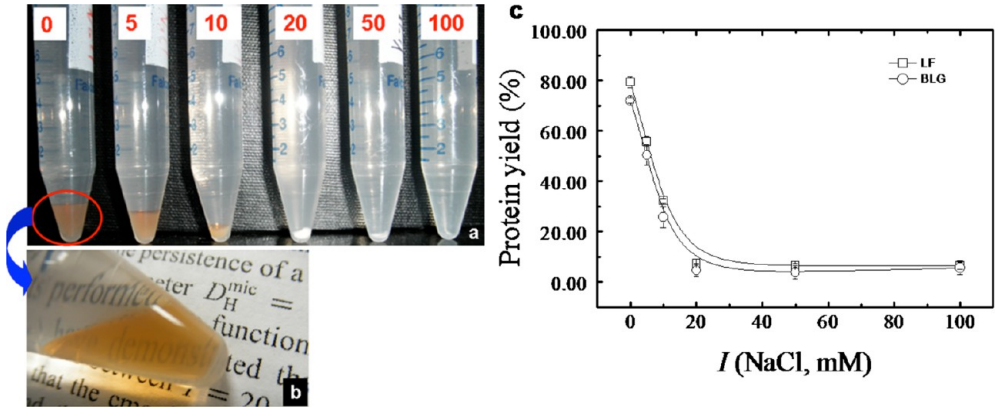

Figure 4. Effect of NaCl (0–100 mM) on BLG–LF (1/1, C_P = 20 g/L, pH 5.9) mixture. BLG and LF solutions were adjusted to desired pH and ionic strength prior to mixing ("pH first"). (a) Observation of the mixture after equilibration and centrifugation; (b) transparence and fluidity of BLG–LF coacervate at 0 mM NaCl; (c) protein yield in BLG–LF dense phase measured by SEC.

dx.doi.org/10.1021/la4027464 | Langmuir 2013, 29, 15614–15623

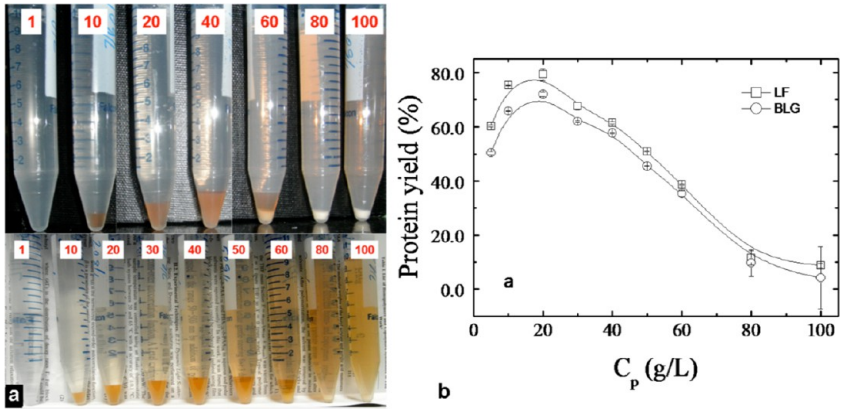

Figure 5. Effect of total protein concentration (1−100 g/L) on BLG−LF (1/1, w/w, pH 6.0, 0 mM NaCl) mixture. (a) Observation of the mixture after equilibration and centrifugation: dark background and light background (with two additional concentrations; 30 g/L and 50 g/L) show more clearly precipitate and supernatant, respectively. (b) Protein yield in BLG−LF dense phase measured by SEC.

concurrence with coacervation has been discussed above in terms of the competition between BLG self-aggregation and complex formation with LF, both pathways open to BLG dimers at 4.0 < pH < 5.5. The shift from the first to the second is reflected in the predominance of coacervation at low salt. The rate of complex formation must be very fast, but the fraction of BLG found in complexes at initial mixing is subject to one or more strongly salt-dependent equilibrium constants, represented in general by K_{BLG-LF}. While ionic strength affects aggregation and complex formation in different ways, it is difficult to distinguish between such kinetic and thermodynamic processes. The dominance of BLG aggregation in the region of intermediate salt is demonstrated when a one-phase solution at I = 100 mM is brought to 5 mM by dialysis against pure water (results not shown). The resemblance of this turbid sample after centrifugation to the "20 mM" tube in Figure 4a confirms that aggregation-induced depletion of free BLG during this high to low salt process effectively competes with higher-order BLG−LF complexation: supernatants obtained at I > 10 mM in Figure 4b showed only $R_h \sim 8$ nm. In contrast, supernatants above coacervates formed from "pH-first" mixing at lower I showed ∼11 nm BLG−LF species. BLG aggregation dominates at higher salt, not because it is intrinsically rapid, but because complex formation is strongly diminished.

Anema and de Kruif[15] recently reported similar I dependence for complex formation in the β-casein/LF system around pH 6.5. However, they obtained complexes up to $I \geq 140$ mM, significantly higher than for BLG−LF. This marked difference might be explained by the random coil structure of β-casein and its relatively high overall hydrophobicity compared to BLG.

3. Effect of Protein Concentration. In Figure 5, coacervate and precipitate both appear at 60 g/L. At higher concentration, only precipitate is seen; at lower concentration, one sees only coacervate in diminishing volumes and finally absent at 1 g/L. The absence of aggregate in the low concentration region is not due solely to the lower concentration of BLG: in the absence of LF, BLG would aggregate strongly under these conditions.[4] Coacervation thus competes with aggregation at $10 < C_P < 40$ g/L. At lower concentrations, that is, 1 g/L, neither precipitation nor coacervation occurs and DLS discloses only 7 nm complexes, probably $LF(BLG_2)$. At C_P > 50 g/L, the coacervation−aggregation competition shifts in favor of BLG aggregation because the rate of aggregation (calculated by a technique described in ref 21) is roughly linear with BLG concentration (data not shown). The disappearance of coacervate could be a direct effect of the depletion of free BLG, but might also be related to self-suppression of coacervation as extensively reported by Overbeek et al.[24] and Veis et al.[25] for polyelectrolyte systems. Self-suppression is thought to occur when complexes overlap at C^* and the entropy gain from coacervation is lost. At these concentrations, DLS shows complexes 11−15 nm, attributable to $LF(BLG_2)_2$. This suggested a complex that differs from $LF(BLG)_4$ because BLG appears to be dimeric at pH 6.0.[4] An approximate calculation for the overlap concentration for R_h = 11 nm complexes with mass of $LF(BLG_2)_2$ (ca. 150 kDa) gives $C^* \sim$ 30 g/L, in rough agreement with the protein concentration at which coacervate yield begins to decline in Figure 5b.

4. Effect of Protein Stoichiometry. Figure 6 shows that maximal coacervation is obtained close to an initial protein

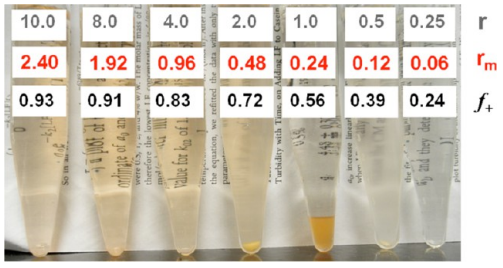

Figure 6. Effect of protein ratio (r = LF/BLG) on BLG−LF mixture (pH 6.0, 0 mM NaCl, C_P = 20 g/L). The molar ratio (r_m) and charge fraction of positive charge relative to total charge (f_+) of LF/BLG are indicated on the tubes. pH adjusted prior to mixing with different volume ratios. The spacing between samples does not provide clear evidence of the range of r leading to coacervation in the vicinity of r = 1.0 (see text for explanation).

stoichiometry that essentially matches that of the coacervate, corresponding on a molar basis to $LF(BLG_2)_2$, i.e., $r = 1.0 \pm 0.3$ (see Figure S2 in the Supporting Information), and to $f_+ = 0.6 \pm 0.04$. BLG aggregation is suppressed by increasing LF concentration (r > 2) and is evident only at r = 2. As noted above, this decrease in aggregation may arise from (1) low BLG bulk concentration (large r) through a purely kinetic effect, as for both tubes 1 and 2 in Figure 5 and tubes 1−4 in Figure 6; or (2) from a low effective BLG concentration, reduced by

dx.doi.org/10.1021/la4027464 | Langmuir 2013, 29, 15614−15623

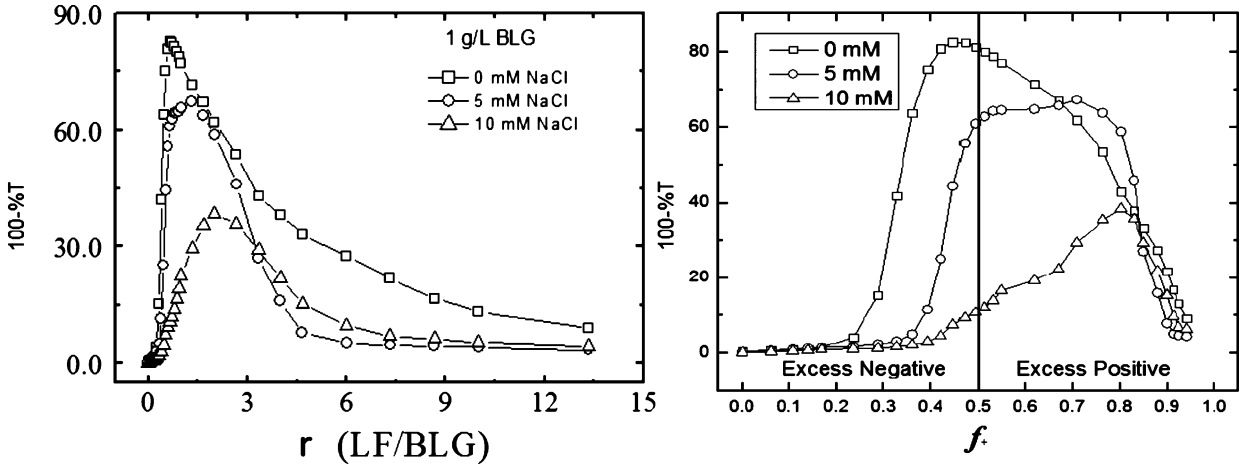

Figure 7. (left) Turbidimetric titration of 1.0 g/L BLG at pH 6.0 with 100 g/L LF in 0−10 mM NaCl. (right) Representation of the left panel with corresponding positive charge fractions of data obtained at 0−10 mM NaCl at pH 6.0.

complexation or coacervation, as in tubes 2−4 in Figure 5 or tube 5 in Figure 6.

Evidence for a decrease in $[BLG]_{eff}$ via complexation by LF was sought in the results of turbidimetric titrations of BLG with LF. These are shown in Figure 7 for the pH and I conditions of Figures 5 and 6, along with results for I = 5 and 10 mM. All data show a sharp increase in turbidity at low r followed by a maximum which coincides with the r = 1 condition of Figure 6. This value of r is equivalent to a BLG:LF ratio of 4:1, corresponding to the $LF(BLG_2)_2$ complex noted in the discussion of Figure 5, implicating this complex as the precursor of the coacervation that leads to high turbidity in Figure 7. The absence of coacervate at identical values of r, I, pH, and C_P in Figure 5 suggests an effect of sample history (mode of addition). The asymmetry of Figure 7 (left) is reduced when the turbidity is plotted versus mole fraction or, in Figure 7 (right), charge fraction. The turbidity maximum at f_+ = 0.46 is lower that the value of $f_+ \sim 0.6$ noted above. This may mean that kinetics of coacervation and coacervate dissolution may play a role in the titration, with the turbidity maxima of Figures 7 corresponding to a condition at which the two rates are turbidimetrically equal. Complexes of LF and BLG at large excess BLG ($r < 0.5$ or $f_+ < 0.2$) are few in number and fail to form higher-order aggregates: evidence for increase in the number of complexes (at fixed stoichiometry) linear with added LF comes from measurements of proton release (not shown here). With increasing r, a transition from $LF(BLG_2)_2$ to $LF(BLG_2)$ or $LF(BLG)_2$ diminishes coacervation, with excess LF eventually inhibiting both coacervation and BLG aggregation as seen for $r > 2$ ($f_+ > 0.6$) in Figure 6 (Scheme 1).

The right panel in Figure 7 shows the "type 2" titration data plotted as a function of positive charge fraction. For no added salt, the maximum turbidity corresponding to $f_+ < 0.5$ is followed by a decrease with addition of excess LF. Excess LF affects the equilibrium between $LF(BLG_2)_2$ and $LF(BLG)_2$ (Scheme 1), shifting it to lower order complexes not eligible for coacervation. The values of [+]/[−] in the Type 2 titration are difficult to interpret, as the addition of LF at pH 6 to BLG at pH 6 significantly lowers the pH, probably due to a pK shift of BLG aspartic acid and glutamic acid residues complexed near the positive domain of LF (Figure S3, Supporting Information). Evidence for complex formation of BLG and LF also comes from the drop by 0.6 pH units when the two proteins are mixed at pH 6 (Figure S3). A variety of complexes are formed, including some with excess LF, but probably the bulk stoichiometry favors $LF(BLG_2)_2$ as the major complex for coacervation.

Scheme 1. Description of the Equilibrium between Complexes, Coacervate, and Individual LF and BLG, and the Kinetics of BLG Self-Aggregation in BLG−LF System

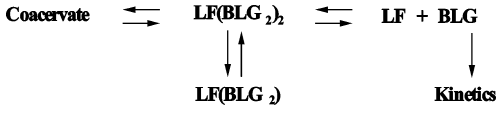

CONDITIONS FOR COACERVATION AND COMPARISON WITH OTHER TYPES OF COACERVATION

1. Conditions for Coacervation. *1.1. Limitations and Phase Boundary.* BLG−LF heteroprotein coacervates are formed under very limited conditions of pH, ionic strength I, total protein concentration C_P, and BLG:LF stoichiometry. The narrow range in which pure (precipitate-free) coacervate could be attained was 5.7 < pH < 6.2, a necessary but not sufficient condition in that the other three variables are also strongly constrained. Other requirements were $0 < I < 20$ mM, $10 < C_P < 40$ g/L, and $0.7 < r < 1.3$ as obtained by separate experiments done at pH 6.0, each with two of the remaining three variables fixed. The results are shown by the surface presented in Figure 8. Although the data points are few, this surface captures some of the salient features of the system: (1) The absence of coacervate at $I > 20$ mM, at $0.7 > r > 1.3$, and at $10 > C_P > 40$ g/L; (2) the symmetrical effect of deviations from r = 1; and (3) the asymmetric effect of deviations from the optimal yield condition of C_P = 20 g/L. The last feature should be expected since the diminution of coacervation at high or low C_P arises from completely different effects: equilibria at low C_P (Results and Discussion, section 1) and self-suppression (see below) at high C_P.

1.2. Structural Implications. The formation of coacervate only in the range near r = 1, and analytical data supporting a similar composition for the coacervate, might be attributed to existence of a well-defined structure of similar molecular stoichiometry. This particular feature of the BLG−LF system

dx.doi.org/10.1021/la4027464 | Langmuir 2013, 29, 15614−15623

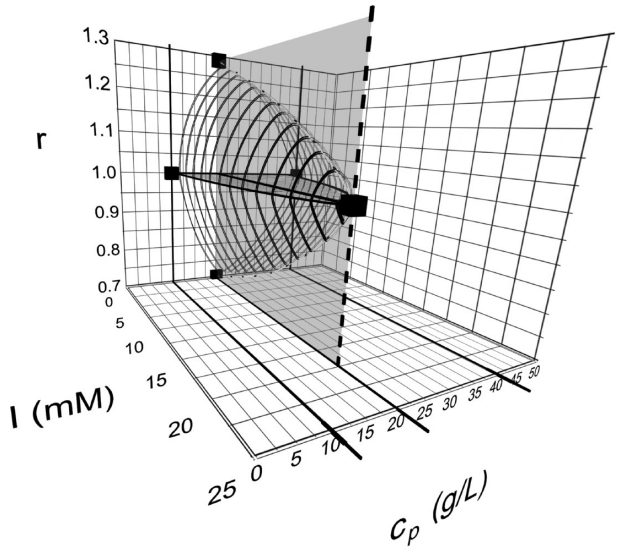

Figure 8. Phase boundaries for the BLG−LF system at pH 6.0. Closed squares (combined with solid black lines) are boundary conditions (obtained from Figures S2 and S4), and the dotted blue line is the trajectory line. Because we use discrete as opposed to continuous experiments, the boundary conditions shown are approximations.

suggests an absence of the disproportionation seen in other types of intermacroionic coacervation,[26,27] as described below. The conditions $r = 1$ and $[+]/[-] = 0.56$ both correspond to $LF(BLG_2)_2$, a structure also consistent with geometric constraint. Bouhallab and co-workers,[1,8−10] considering proteins as spheres, also suggest the importance of both geometry (relative sizes of the two proteins) and charge stoichiometry. Attempts to determine whether charge stoichiometry alone was sufficient for coacervation, by varying r and pH independently to reach the desired value of f_+, were impeded by BLG aggregation. Clearly, structures such as $LF(BLG_2)_2$ are reasonable only for certain protein dimensions. Other systems may not coacervate without a comparable species acting as a near-neutral "primary unit" that can exhibit short-range attractive interactions with other "primary units".

2. Comparison with PE−Micelle and PE−Protein Coacervation. Based on our knowledge, this is the first report on globular protein−protein coacervation with straightforward evidence for liquid−liquid phase separation. Comparing this new model system to well-known other systems: PE−protein and PE−micelle provides better understanding of unique features of heteroprotein coacervation. Several features of BLG−LF coacervation distinguish it from the coacervation behavior of the other two principal classes of macroion coacervation: polyanion−polycation and polyelectrolyte−colloid, the latter mainly represented in the literature by polyelectrolyte−protein and polyelectrolyte−micelle. First, coacervation for BLG−LF is easily suppressed by salt: no coacervation is observed at $I > 20$ mM, while coacervation can typically be observed up to several hundred mM for the other two classes. Second, coacervation for BLG−LF is strongly constrained by macroion stoichiometry, that is, close to a weight ratio of 1:1 ($r = 0.7−1.3$). In contrast, the range of coacervation conditions is $5 < r < 9$ for a polycation−protein system,[28] $2 < r < 3$ for a polycation−micelle system;[29] and even wider for polyanion−polycation systems.[30] The compositional polydispersity of systems can facilitate the exchange of polymers or colloids among complexes, allowing them to attain charge neutrality and thus phase separate. This process, called disproportionation, enables a system with bulk charge stoichiometry $[+]/[-] \neq 1$ to form neutral complexes which then coacervate.[26,27] Further comparisons are introduced below are based on phase boundaries for polyelectrolyte−colloid systems, since well-defined transitions to biphasic states are quite difficult to observe for polyelectrolyte−polyelectrolyte systems, presumably because they are complicated by the typically heterogeneous nature of the polymers used and because rapid association kinetics complicate equilibrium approaches to phase separation.

2.1. Comparison with PE−Micelle System. In one respect, the limitation of the coacervation region to C_P <40 g/L (Figure 5) qualitatively resembles the self-suppression observed for polycation−micelle solutions[31] and polyanion−polycation systems.[7] Figure 9 compares self-suppression conditions for

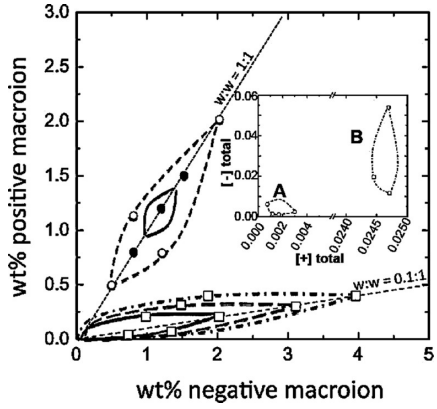

Figure 9. Phase boundaries for LF/BLG at pH 6.0, $I = 0$ (upper) are compared with PDADMAC/SDS-TX100 (lower), an analogous macrocation/macroanion system, as wt % of LF or PDADMAC versus wt % of BLG or SDS-TX100. For LF/BLG, open circles are boundary conditions (obtained from Figures S2 and S4, Supporting Information) and closed circles are conditions known to be within the two-phase region. The solid line is a speculative boundary for $I = 10$ mM. For PDADMAC/SDS-TX100 (open squares), boundary conditions are shown at $T = 42$ °C (solid line), 44 °C (dashed line), and 46 °C (dashed-dotted line). Inset: total [−] versus total [+] for the systems (A) LF/BLG and (B) PDADMAC/SDS-TX100 at $T = 46$ °C. w:w represents the weight percent of positive macroion to negative macroion.

BLG−LF with parallel results for the polycation−micelle system (adapted from ref 31). In both cases, at a fixed stoichiometry, the two-phase region vanishes at high total concentration: the coacervation region depends on both total macroion (movement along diagonals) and macroion ratios (vertical or horizontal motion). The ordinate shows the weight concentrations w of the analogous positively charged macroions (LF and PDADMAC), and the abcissa shows w for the two negatively charged macroions (BLG and SDS/TX100 micelles). Self-suppression is observed when the concentrations of the two macroanions are 20 g/L for BLG and 40 g/L for micelle. The width of the BLG−LF system (upper boundary) is controlled by ionic strength, and the width of the polycation−micelle system (lower boundaries) by temperature. T and I have been closely linked in the polycation−micelle system, an association alluded to in related studies.[30] In the polycation−micelle system, the surface charge density of the micelle required for coacervate formation decreases with either

dx.doi.org/10.1021/la4027464 | Langmuir 2013, 29, 15614−15623

increasing T or decreasing I.[5] The shift toward coacervation at low I arises from an entropy increase due to release of bound counterions, a contribution to the free energy of coacervation obviously amplified by temperature. Thus broadening of the two-phase region with increasing temperature for the polyelectrolyte-micelle system is analogous to broadening of the two-phase BLG−LF coacervation region with decreasing ionic strength. The two sets of closed loops show greater convergence when weight ratios are replaced by the more fundamental charge stoichiometry (inset of Figure 9). On the other hand, coacervation vanishes at low macroion concentration only for BLG−LF.

2.2. Comparison with PE−Protein System. More direct comparisons with BLG−LF would seem more feasible for protein−PE systems in that experimental variables for both systems are pH, I, and stoichiometry. For the protein−PE system, "stoichiometry" can refer to either the mixing ratio of colloid/polymer (bulk) or the ratio of colloid/polymer within the complex (micro). Figure 10 presents results for

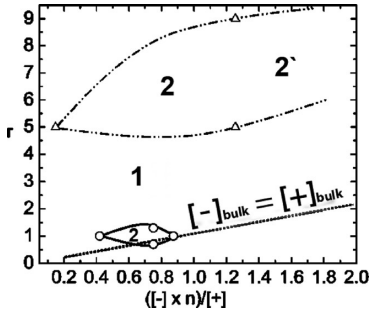

Figure 10. Phase boundaries for BSA-PDADMAC at I = 10 mM, 5.0 < pH < 9.0 (upper) and BLG−LF at I = 0, pH 6.0 (lower), in terms of complex charge ratio and weight ratio r. Z_- represents the charge on anionic BSA and BLG, respectively, and Z_+ the molecular charge on cationic PDADMAC and LF, respectively. The dotted diagonal for BLG−LF represents [−]/[+] = 1. The dashed-dotted line for BSA-PDADMAC is drawn from three existing data points (ref 28). The biphasic region (2) contains for BSA-PDADMAC at high pH precipitate (2′) as well as coacervate.

PDADMAC-BSA for which the coacervation regime can be transited by varying stoichiometry r at fixed pH (see Figure 8, ref 28). To describe the charge state of the primary unit for BLG−LF coacervation, we can use $n(Z_-/Z_+)$, where n = 4, [−] is the pH-dependent charge of BLG, and [+] is the pH-dependent charge of LF. The complex charge ratio for both systems is represented on the abscissa by $n(Z_-/Z_+)$, where Z_- represents the net charge on BLG or BSA, [+] represents the charge of LF or of one PDADMAC chain, and n is the complex molar stoichiometry, that is, n = 4:1 for $LF(BLG_2)_2$ or 120:1 for BSA/PDADMAC. The deviation of "bulk" stoichiometry from the "micro" stoichiometry could result in a two-phase region for PDADMAC-BSA very far from the [−]/[+] = 1 line (not shown on the plot). It is however clear that the coacervation region is very broad for PDADMAC-BSA, possibly because disproportionation allows for formation of complexes that are able to coacervate when the system is far from charge neutrality bulk, that is, [−]/[+] is far from 1.

CONCLUSIONS

Heteroprotein coacervation between BLG and LF occurs at highly specific conditions of pH, ionic strength, total protein concentration, and protein stoichiometry. While these variables also control protein−polyelectrolyte coacervation, they are more highly restricted for BLG−LF coacervation. To a considerable degree, BLG−LF coacervation is obscured or inhibited by rapid BLG self-association, because the pH/I conditions for coacervation include regions in which BLG aggregation competes with BLG−LF complex formation. DLS measurements in the one-phase regime, and analysis of coacervates, suggest that the $LF(BLG_2)_2$ complex might be the primary unit of the 1:1 w:w BLG:LF coacervate. Such units might interact through short-range electrostatic attraction between the respective negative and positive surface domains of BLG and LF, respectively, in combination with weaker interprimary unit repulsive forces. Entropic forces related to counterion release are significantly diminished relative to polyelectrolyte-based systems, due to the relatively low charge densities for BLG−LF, while effects due to chain configurational entropy are absent in the globular heteroprotein system. In addition, compositional analysis supports a similar composition for both the coacervate and the one-phase systems, which might be attributed to the existence of a well-defined structure of similar molecular stoichiometry. Therefore, disproportionation[25,26] through which some complexes may coacervate, while others are left behind in the supernatant, is very unlikely. The limited conditions for heteroprotein coacervation might thus reflect its reliance on enthalpic contributions. We will focus on the thermodynamics of heteroprotein coacervation in another paper in preparation. The microstructure of the BLG−LF coacervate is currently under investigation by SANS and rheology to identify the structure of the elementary stoichiometric units suggested at present.

ASSOCIATED CONTENT

Supporting Information

Additional figures as described in the text. This material is available free of charge via the Internet at http://pubs.acs.org.

AUTHOR INFORMATION

Corresponding Authors

*E-mail: ekizilay@chem.umass.edu.
*E-mail: dubin@chem.umass.edu.

Notes

The authors declare no competing financial interest.

ACKNOWLEDGMENTS

We acknowledge the support of NESTEC and of the National Science Foundation (CBET-0966923 and 1133289).

REFERENCES

(1) Desfougeres, Y.; Croguennec, T.; Lechevalier, V.; Bouhallab, S.; Nau, F. Charge and size drive spontaneous self-assembly of oppositely charged globular proteins into microspheres. *J. Phys. Chem. B* **2010**, *114* (12), 4138−4144.

(2) Nigen, M.; Croguennec, T.; Bouhallab, S. Formation and stability of alpha-lactalbumin-lysozyme spherical particles: Involvement of electrostatic forces. *Food Hydrocolloids* **2009**, *23* (2), 510−518.

(3) Hwang, D.; Zeng, H.; Srivastava, A.; Krogstad, D. V.; Tirrell, M.; Israelachvili, J. N.; Waite, J. H Viscosity and interfacial properties in a mussel-inspired adhesive coacervate. *Soft Matter* **2010**, *6* (14), 3232−3236.

(4) Mahji, P.; Ganta, R. R.; Vanam, R. P.; Seyrek, E.; Giger, K.; Dubin, P. L. Electrostatically driven protein aggregation: b-

lactoglobulin at low ionic strength. *Langmuir* **2006**, *22* (22), 9150−9159.
(5) Kumar, A.; Dubin, P. L.; Hernon, M. J.; Li, Y.; Jaeger, W. Temperature-dependent phase behavior of polyelectrolyte - mixed micelle systems. *J. Phys. Chem. B* **2007**, *111* (29), 8468−8476.
(6) Kizilay, E.; Kayitmazer, A. B.; Dubin, P. L. Complexation and coacervation of polyelectrolytes with oppositely charged colloids. *Adv. Colloid Interface Sci.* **2011**, *167* (1−2), 24−37.
(7) Veis, A. A review of the early development of the thermodynamics of the complex coacervation phase separation. *Adv. Colloid Interface Sci.* **2011**, *167* (1−2), 2−11.
(8) Salvatore, D. B.; Duraffourg, N.; Favier, A.; Persson, B. A.; Lund, M.; Delage, M.-M.; Silvers, R.; Schwalbe, H.; Croguennec, T.; Bouhallab, S.; Forge, V. Investigation at Residue Level of the Early Steps during the Assembly of Two Proteins into Supramolecular Objects. *Biomacromolecules* **2011**, *12* (6), 2200−2210.
(9) Salvatore, D.; Croguennec, T.; Bouhallab, S.; Forge, V.; Nicolai, T. Kinetics and Structure during Self-Assembly of Oppositely Charged Proteins in Aqueous Solution. *Biomacromolecules* **2011**, *12* (5), 1920−1926.
(10) Nigen, M.; Le Tilly, V.; Croguennec, T.; Drouin-Kucma, D.; Bouhallab, S. Molecular interaction between apo or holo alpha-lactalbumin and lysozyme: Formation of heterodimers as assessed by fluorescence measurements. *Biochim. Biophys. Acta, Proteins Proteomics* **2009**, *1794* (4), 709−715.
(11) Howell, N. K.; Yeboah, N. A.; Lewis, D. F. V. Studies on the electrostatic interactions of lysozyme with alpha-lactalbumin and beta-lactoglobulin. *Int. J. Food Sci. Technol.* **1995**, *30* (6), 813−824.
(12) Takase, K. Reactions of denatured proteins with other cellular components to form insoluble aggregates and protection by lactoferrin. *FEBS Lett.* **2008**, *441*, 271−274.
(13) Howlett, G. J.; Nichol, L. W. Sedimentation Equilibrium Study of Interaction between Ovalbumin and Lysozyme. *J. Biol. Chem.* **1973**, *248* (2), 619−621.
(14) Tiwari, A.; Bindal, S.; Bohidar, H. B. Kinetics of protein-protein complex coacervation and biphasic release of salbutamol sulfate from coacervate matrix. *Biomacromolecules* **2009**, *10* (1), 184−189.
(15) Anema, S. G.; de Kruif, C. G. Co-acervates of lactoferrin and caseins. *Soft Matter* **2012**, *8*, 4471−4478.
(16) Anema, S. G.; de Kruif, C. G. Interaction of lactoferrin and lysozyme with casein micelles. *Biomacromolecules* **2011**, *12*, 3970−3976.
(17) Abril Garcia-Montoya, I.; Siqueiros Cendon, T.; Arevalo-Gallegos, S.; Rascon-Cruz, Q. Lactoferrin a multiple bioactive protein: An overview. *Biochim. Biophys. Acta, Gen. Subj.* **2012**, *1820* (3), 226−236.
(18) Mao, Y.; McClements, D. J. Modulation of bulk physicochemical properties of emulsions by hetero-aggregation of oppositely charged protein-coated lipid droplets. *Food Hydrocolloids* **2011**, *25* (5), 1201−1209.
(19) Farnaud, S.; Evans, R. W. Lactoferrin - a multifunctional protein with antimicrobial properties. *Mol. Immunol.* **2003**, *40* (7), 395−405.
(20) Nicolai, T.; Britten, M.; Schmitt, C. b-Lactoglobulin and WPI aggregates: Formation, structure and applications. *Food Hydrocolloids* **2011**, *25*, 1945−1962.
(21) Yan, Y.; Seeman, D.; Zheng, B.; Kizilay, E.; Xu, Y.; Dubin., P. L. pH-Dependent Aggregation and Disaggregation of Native *β*-Lactoglobulin in Low Salt. *Langmuir* **2013**, *29* (14), 4584−4593.
(22) Schmitt, C.; Sanchez, C.; Despond, S.; Renard, D.; Thomas, F.; Hardy, J. Effect of protein aggregates on the complex coacervation between b-lactoglobulin and acacia gum at pH 4.2. *Food Hydrocolloids* **2000**, *14* (3), 403−413.
(23) Schmitt, C.; Sanchez, C.; Lamprecht, A.; Renard, D.; Lehr, C.-M.; de Kruif, C. G.; Hardy, J. Study of B-lactoglobulin-acacia gum complex coacervation using diffusing wave spectroscopy and confocal laser scanning microscopy. *Colloids Surf., B* **2001**, *20* (3), 267−280.
(24) Michaeli, I.; Overbeek, J. T. G.; Voorn, M. J. Phase Separation of Polyelectrolyte Solutions. *J. Polym. Sci.* **1957**, *23* (103), 443−450.
(25) Veis, A.; Bodor, E.; Mussell, S. Molecular weight fractionation and self-suppression of complex coacervation. *Biopolymers* **1967**, *5* (1), 3.
(26) Kizilay, E.; Maccarrone, S.; Foun, E.; Dinsmore, A. D.; Dubin, P. L. Cluster formation in polyelectrolyte-micelle complex coacervation. *J. Phys. Chem. B* **2011**, *115* (22), 7256−7263.
(27) Zhang, R.; Shklovskii, B. T. Phase diagram of solution of oppositely charged polyelectrolytes. *Phys. A* **2005**, *352* (1), 216−238.
(28) Antonov, M.; Mazzawi, M.; Dubin, P. L. Entering and exiting the protein-polyelectrolyte coacervate phase via nonmonotonic salt dependence of critical conditions. *Biomacromolecules* **2010**, *11* (1), 51−59.
(29) Wang, Y. L.; Kimura, K.; Dubin, P. L.; Jaeger, W. Polyelectrolyte-micelle coacervation: effects of micelle surface charge density, polymer molecular weight, and polymer/surfactant ratio. *Macromolecules* **2000**, *33* (9), 3324−3331.
(30) Spruijt, E.; Sprakel, J.; Lemmers, M. Relaxation Dynamics at Different Time Scales in Electrostatic Complexes: Time-Salt Superposition. *Phys. Rev. Lett.* **2010**, *105* (20), 208301−208304.
(31) Li, Y.; Dubin, P.; Havel, H. A.; Edwards, S. L.; Dautzenberg, H. Complex formation between polyelectrolyte and oppositely charged mixed micelles: soluble complexes vs coacervation. *Langmuir* **1995**, *11* (7), 2486−2492.

NOTE ADDED AFTER ASAP PUBLICATION

This paper was published on the Web on December 4, 2013, with the incorrect TOC and Abstract graphics. The corrected version was reposted on December 6, 2013.